Nanofabrication of photonic crystal membrane lasers

Reference 69

J. R. Cao,[a] Po-Tsung Lee, Sang-Jun Choi, Roshanak Shafiiha, Seung-June Choi, John D. O'Brien, and P. Daniel Dapkus
Department of EE Electrophysics, University of Southern California, PHE 424, 3737 Watt Way, Los Angeles, California 90089

(Received 19 July 2001; accepted for publication 14 January 2002)

We present techniques for fabricating photonic crystal (PC) membrane defect lasers. These nanostructures operate as optically pumped lasers under pulsed conditions at room temperature. The thin membrane PC defect structures are formed by transferring an electron-beam lithographically defined lattice pattern into an epitaxial layer structure by a sequential process of ion beam etching, reactive ion etching, and electron cyclotron resonance etching steps. A V-shape undercut channel is formed by a wet chemical etching using a 4:1 mixture of HCl and H_2O to create the suspended membrane. We include a detailed description of a dependable and repeatable HCl undercut process for the PC structure. © *2002 American Vacuum Society.* [DOI: 10.1116/1.1458951]

I. INTRODUCTION

The design and fabrication of photonic crystal (PC) structures in semiconductors has been gaining increased attention since their theoretical prediction[1] and experimental realization.[2] With the assistance of numerical simulation,[3] it is possible to design a wide range of high performance PC devices, such as compact filters,[4] reflectors, sharp bending waveguides,[5] and microscale lasers,[2] some of which we will report in this article. With these state-of-the-art devices that tailor electromagnetic fields at the submicron scale, it should be possible to produce integrated PC circuits in the near future.

In this article, we present a detailed description of a complete process to fabricate membrane PC defect lasers. The membrane is formed to provide strong optical confinement in the normal direction. These structures are fabricated in InGaAsP epitaxial layers containing quantum wells on an InP substrate.[6]

II. FABRICATION PROCEDURE

The structure of interest in this article is shown in Fig. 1(a). It consists of a 224 nm membrane suspended in air, with a two-dimensional triangular PC lattice defining a laser cavity etched through the membrane. The epitaxial layers of the membrane were deposited by metalorganic chemical vapor deposition. The epitaxial structure is shown in Fig. 1(b). The membrane contains four 1.2% compressively strained InGaAsP quantum wells separated by 23 nm unstrained InGaAsP barrier layers. The photoluminescence spectrum of these quantum wells shows emission between 1420 and 1630 nm and is peaked at 1.5 μm at room temperature. On top of the last barrier layer, a 60 nm InP layer is grown to protect the quantum wells during the dry etching steps. The InP cap layer is subsequently removed at the end of the device processing.

After the epitaxial growth, an etch mask is deposited on the sample. This mask consists of 160 nm of plasma-enhanced chemical vapor deposition silicon nitride with 5 nm of Cr and 45 nm of Au deposited by e-beam evaporation. Finally, a 100 nm 2% polymethylmethacrylate (PMMA) layer is deposited by spin coating.

The PC pattern is defined in the PMMA by electron beam lithography. This is done in a modified Philips XL30 scanning electron microscope. We have written both triangular lattice and square lattice PCs with lattice constants ranging from 460 to 560 nm, and with the r/a ratio varying from 0.21 to 0.42. Here, r is the hole radius, and a is the PC lattice constant. The PMMA is developed for 50 s in a 3:7 mixture of 2-ethoxyethanol and methanol. A typical pattern after electron beam lithography is shown in Fig. 2(a).

After lithography, the pattern is transferred into the Cr/Au metal layer by Ar^+ milling in an ion beam etching (IBE) system. The ion accelerating voltage in the IBE is 500 V. The patterned Cr/Au layer is then used as a mask to pattern the silicon nitride layer by CF_4 dry etching in a reactive ion etching (RIE) system. Figures 2(b) and 2(c) are a side view and a top view, after the RIE etching. At this stage, we have a sharply defined and robust mask for the next electron cyclotron resonance (ECR) etching step.

The pattern is then transferred 400 nm deep into the semiconductor using ECR etching. The gas mixture used in this etch is 38/24/12 sccm $CH_4/H_2/Ar$. The rf power is set to 300 W and the microwave power is set to 600 W. This etch recipe was developed to produce high aspect ratio structures. The etch rate in the ECR is about 1 nm/s for our feature size. By the time ECR etching is done, the metal layer has been completely removed. During this process, we use RIE oxygen plasma to clean the excessive polymer on the sample that is generated by CH_4 chemistry after every 200 s of ECR etch. A cross section for a typical sample after this ECR etch is shown in Fig. 2(d). The selectivity of our SiN_x mask to InP is about 1:6 for the combined ECR and oxygen plasma etch.

After the metal layer is removed, the sample is then etched again by RIE to completely remove the silicon–nitride mask using the CF_4 plasma.

[a]Author to whom correspondence should be addressed; electronic mail: caoj@usc.edu

Report Documentation Page

Form Approved
OMB No. 0704-0188

1. REPORT DATE	2. REPORT TYPE	3. DATES COVERED
01 JUN 2005	**N/A**	**-**

4. TITLE AND SUBTITLE	5a. CONTRACT NUMBER
Nanofabrication of photonic crystal membrane lasers	5b. GRANT NUMBER
	5c. PROGRAM ELEMENT NUMBER
6. AUTHOR(S)	5d. PROJECT NUMBER
	5e. TASK NUMBER
	5f. WORK UNIT NUMBER
7. PERFORMING ORGANIZATION NAME(S) AND ADDRESS(ES) **Department of EE Electrophysics, University of Southern California, PHE 424, 3737 Watt Way, Los Angeles, California 90089**	8. PERFORMING ORGANIZATION REPORT NUMBER
9. SPONSORING/MONITORING AGENCY NAME(S) AND ADDRESS(ES)	10. SPONSOR/MONITOR'S ACRONYM(S)
	11. SPONSOR/MONITOR'S REPORT NUMBER(S)

12. DISTRIBUTION/AVAILABILITY STATEMENT
Approved for public release, distribution unlimited

13. SUPPLEMENTARY NOTES
See also ADM001923.

14. ABSTRACT

15. SUBJECT TERMS

16. SECURITY CLASSIFICATION OF:			17. LIMITATION OF ABSTRACT	18. NUMBER OF PAGES	19a. NAME OF RESPONSIBLE PERSON
a. REPORT	b. ABSTRACT	c. THIS PAGE			
unclassified	**unclassified**	**unclassified**	**UU**	**4**	

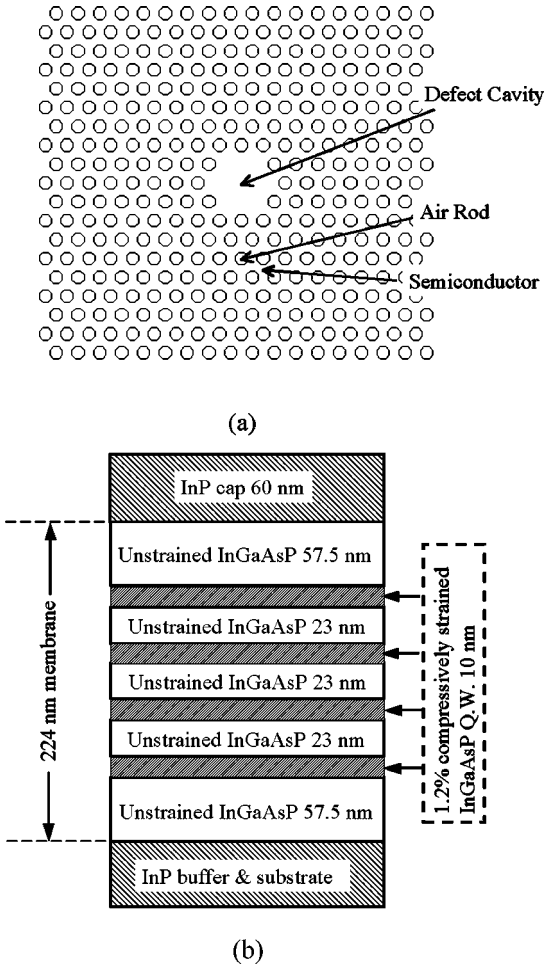

FIG. 1. (a) PC membrane defect structure and (b) epitaxial structure.

The final step is a wet chemical etching, which undercuts the membrane and strips the 60 nm InP cap layer to achieve a smooth surface. This process also smoothes most of the sharp features on the sidewalls of the holes, which decreases the optical loss caused by the roughness. We have, however, no practical method to measure this improvement quantitatively at this point. The wet etching is done at 0 °C in a $HCl:H_2O=4:1$ mixture. This wet etching is anisotropic[7] and this has important consequences in the fabrication of undercut photonic crystal membranes. For example, attention must be paid to the orientation of triangular lattice PCs.

The consequences of this anisotropy can be seen in Fig. 3(a), i.e., the chemical etch stops at certain slow etching planes for $HCl:H_2O=4:1$ at 0 °C. The etching results in a wedge-shaped profile for a square pattern. Figure 3(a) shows that the HCl etching effectively stops at 95° and 40° from the $\langle -1,0,0\rangle$ direction in the $(0,-1,-1)$ plane and the $(0,1,-1)$ planes, respectively. The roughness that appears on the 40° planes, whose normal direction lies in the $(0,1,-1)$ plane, is also consistent with the fact that the etching rate is near zero in a large range of angles around this direction. Therefore, surface features on this etch-stop plane are removed very slowly. More details on these etch-stop planes can be found in Ref. 7.

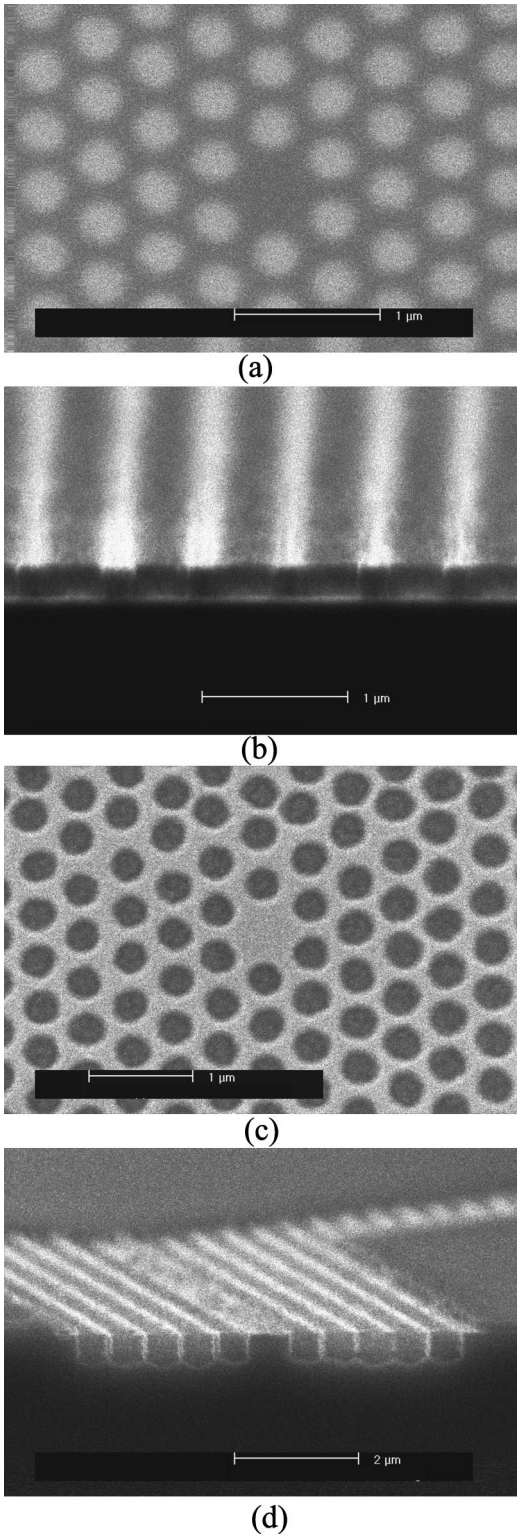

FIG. 2. PC structure after: (a) electron-beam lithography, (b) CF_4 RIE etch through silicon nitride (cross section), (c) CF_4 RIE etch through silicon nitride (top view), and (d) $CH_4/H_2/Ar$ ECR etch into InGaAsP and InP.

Similar results occurred in the etching of PC waveguides. As shown in Fig. 3(b), the wet undercut etching of this PC waveguide (square lattice) results in a small wedge-shape hole in each PC hole. After 30 min of etching, no undercut is

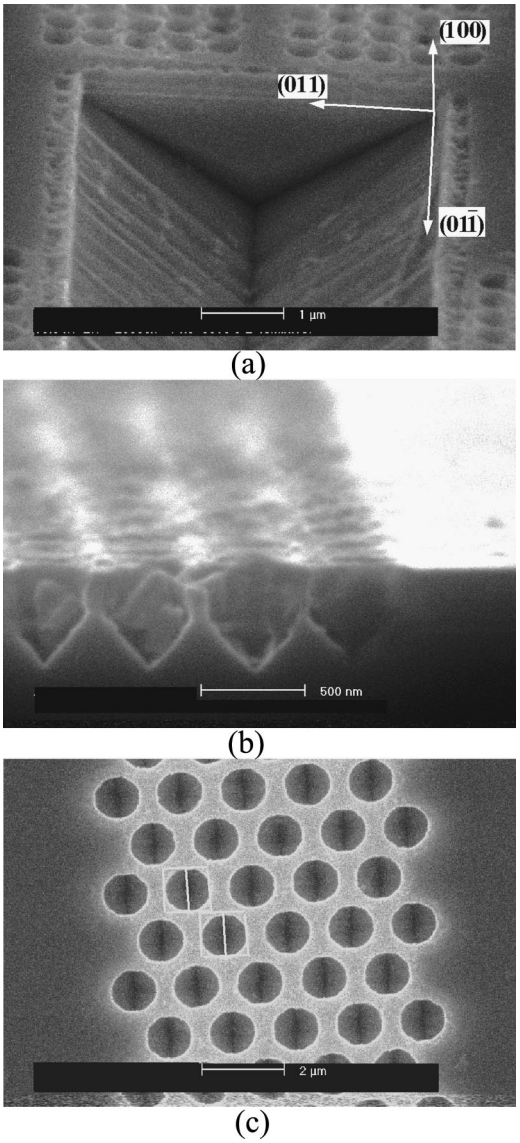

FIG. 3. (a) ''Wedge'' formed by etching stop planes; (b) small ''wedges'' formed in PC; and (c) small ''wedges'' under those holes, which have some chance to meet at the corner in this case.

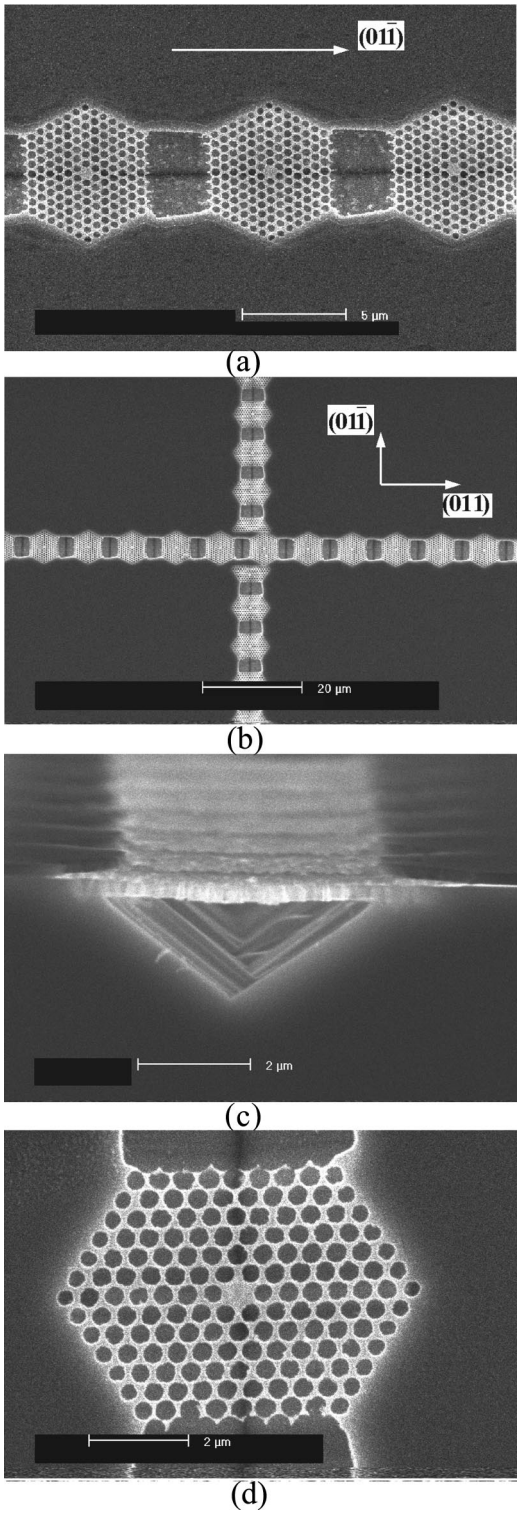

FIG. 4. (a) Opening areas at the ends of PC structures along the $\langle 0,1,-1\rangle$ direction, (b) dozens of PC structures aligned in one trench, (c) the V-shape undercut passing through 28 PC defect structures (cross section), and (d) final defect structure.

formed. This occurs even though the etching speed in the $\langle -1,0,0\rangle$ direction is about 1 μm/min[8] on unpatterned substrates. The reason is that the etching speed between 95° and 140° is practically zero, in the (0,1,1) plane. The HCl etching stops when it reaches 95° in the (0,1,1) plane [or 40° in the $(0,1,-1)$ plane].

These etch-stop plane can be avoided if the *r/a* ratio is large, and the triangular lattice is oriented along $\langle 0,1,1\rangle$, as shown in Fig. 3(c). Figure 3(c) shows that the underlying wedges (delineated by white lines) can meet each other at the corners of the etched feature in this case. Once they meet, the etch-stop planes are broken, and the HCl etching can proceed quickly in all directions to remove the underlying InP. However, in some cases, the HCl etching will be limited by the etch-stop planes and the undercut will not proceed. This happens when the triangular lattice photonic crystal is oriented along the $\langle 0,1,-1\rangle$ direction, or when square lattice PCs are fabricated, or when the PC structures have a small *r/a* ratio. For these cases, the small wedges under every hole have no chance to meet each other. Hence, no undercut can be formed.

A solution for this problem that is effective for all types of

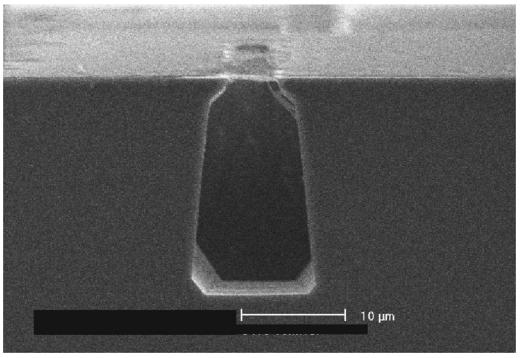

FIG. 5. Cross section of a ⟨0,1,1⟩ arm that is undercut.

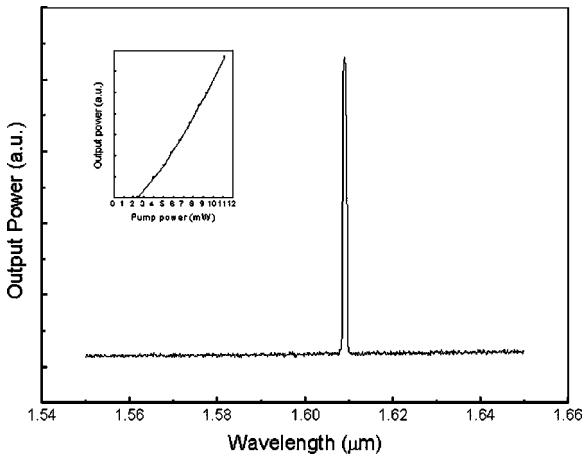

FIG. 6. Optical spectrum of a photonic crystal membrane defect laser and pumping input vs optical characteristics (inset).

PC lattices, regardless of the relative orientation to the InP crystal, is to form large openings at the ends of the pattern merging into the edges of the PC along the ⟨0,1,−1⟩ orientation, as shown in Fig. 4(a). Owing to their dramatically different physical dimensions compared with the PC holes and their asymmetric shape, these opening windows prevent the etch-stop planes from forming. Figure 4(b) shows several PC patterns aligned in one long trench.

The chemical etching can now undercut the PC area from the window areas. Because of the window area, it is almost impossible to form etch-stop plane at the merging interface. Since the etch-stop planes are not formed, the undercut proceeds along ⟨0,1,−1⟩ orientation at a high rate. (The etch rate is maximum at 70°–90°.[7]) Within 10 min, a perfect V-shape undercut trench is formed, passing through 28 PC structures [Fig. 4(c)].

This etching with $HCl:H_2O=4:1$ at 0 °C can be done in a few minutes depending on how far the undercut needs to go between the two windows. Using this undercut technique, complete undercut of the triangular lattice with an *r/a* ratio as small as 0.21 has been achieved.

We also note that the trench along the ⟨0,1,1⟩ direction, i.e., the horizontal arm of the cross in Fig. 4(b), can also be undercut in some cases. Once the trench is formed, the etch can go very deep in a short time. Figure 5 shows the cross section for a ⟨0,1,1⟩ arm. The etch depth after 10 min is over 15 μm. This image also shows the θ_1, θ_2, and θ_3 etch-stop planes, which were observed in Ref. 7. We do not recommend aligning the PCs along the ⟨0,1,1⟩ direction, however, because it is more difficult to undercut than the ⟨0,1,−1⟩ direction. Figure 4(d) shows the final structure for a defect laser structure.

With the process above, optically pumped laser structures with threshold pump powers of less than 3 mW have been demonstrated in cavities formed by removing 19 holes from the lattice. Figure 6 shows the optical spectrum and output power versus input power curve from one of these lasers. Pulsed operation with pulses longer than 100 ns and duty cycle larger than 5%, has also been achieved at room temperature. The smallest defect structures from which we have observed lasing at room temperature are cavities formed by removing 13 holes from the PC lattice. We have not yet achieved lasing in smaller resonant cavities. We attribute this to an inability to focus our multimoded vertical cavity surface emitting laser pump laser to a smaller spot size.

III. CONCLUSION

We have presented a reliable fabrication process for PC membrane defect lasers that have excellent performance at room temperature. We have also shown a study of the HCl wet chemical etching process, which is crucial for making a dependable undercut and smooth surfaces. The V-shape undercut strategy enables us to make a large variety of different structures without worrying about whether we are fabricating triangular lattices, or whether the PC has a large *r/a* ratio.

ACKNOWLEDGMENTS

This article is based upon work supported in part by the U.S. Army Research Laboratory and the Army Research Office under Contract No. DAAD 19-99-0121 and in part by the Defense Advanced Research Projects Agency under Contract Nos. MDA972-00-1-0019 and N00014-00-C-8079.

[1]E. Yablonovitch, Phys. Rev. Lett. **58**, 2059 (1987).
[2]O. Painter, R. K. Lee, A. Scherer, A. Yariv, J. D. O'Brien, P. D. Dapkus, and I. Kim, Science **284**, 1819 (1999).
[3]O. Painter, J. Vuckovic, and A. Scherer, J. Opt. Soc. Am. B **275**, 16 (1999).
[4]S. Fan, P. R. Villeneuve, J. D. Joannopoulos, and H. A. Haus, Phys. Rev. Lett. **80**, 960 (1998).
[5]M. Loncar, D. Nedelijkovic, T. Doll, J. Vuckovic, A. Scherer, and T. P. Pearsall, Appl. Phys. Lett. **77**, 1937 (2000).
[6]I. Kim, D. G. Chang, and P. D. Dapkus, J. Cryst. Growth **119**, 138 (1988).
[7]L. A. Coldren, K. Furuya, and B. I. Miller, J. Electrochem. Soc. **31**, 1918 (1983).
[8]Y. Suematsu and A. R. Adams, *Handbook of Semiconductor Lasers and Photonic Integrated Circuits* (Chapman & Hall, London, 1994), p. 498.